

Communication

High-Order Harmonics Generation in Atomic and Molecular Zinc Plasmas

Rashid A. Ganeev^{1,2,3,*}  and Hiroto Kuroda^{1,4,5}

¹ Ophthalmology and Advanced Laser Medical Center, Saitama Medical University, Saitama 350-0495, Japan; cd838737@wj8.so-net.ne.jp

² Institute of Astronomy, University of Latvia, Riga LV-1586, Latvia

³ Department of Physics, Voronezh State University, 394006 Voronezh, Russia

⁴ Advanced Laser Technology Inc., Tokyo 206-0014, Japan

⁵ Plasma Investigations Group, Aichi Medical University, Nagakute 480-1195, Japan

* Correspondence: rashid_ganeev@mail.ru

Abstract: We demonstrate the variations of single harmonic resonance enhancement during high-order harmonics generation in zinc-containing atomic and molecular species at the conditions of single-color and two-color pumps of laser-induced plasmas by applying different laser sources. We show how selenides of this metal notably modify the enhancement of single (9th, 15th or 16th) harmonic compared with purely atomic zinc plasmas. The variations of single harmonic enhancement are demonstrated using fixed (806 nm) and tunable (1280–1440 nm) radiation.

Keywords: zinc-contained plasma; high-order harmonics; resonance enhancement



Citation: Ganeev, R.A.; Kuroda, H. High-Order Harmonics Generation in Atomic and Molecular Zinc Plasmas. *Photonics* **2021**, *8*, 29. <https://doi.org/10.3390/photonics8020029>

Received: 2 January 2021

Accepted: 21 January 2021

Published: 25 January 2021

Publisher's Note: MDPI stays neutral with regard to jurisdictional claims in published maps and institutional affiliations.



Copyright: © 2021 by the authors. Licensee MDPI, Basel, Switzerland. This article is an open access article distributed under the terms and conditions of the Creative Commons Attribution (CC BY) license (<https://creativecommons.org/licenses/by/4.0/>).

1. Introduction

Although the generation of high-order harmonics due to the interaction of intense laser pulses with matter provides a unique source of coherent femtosecond and attosecond pulses in the extreme ultraviolet range (XUV), the low efficiency of this process ($<10^{-6}$) is a serious disadvantage for its wide application. To increase the efficiency of high-order harmonic generation (HHG), various methods have been introduced, in particular, resonance-induced amplification, especially in the case of their generation in laser-induced plasma (LIP) formed during laser ablation of solids. The resonance-induced amplification of a single harmonic is attributed to the proximity of the autoionizing states (AIS) of single-charged ions and some specific harmonic orders [1–3]. Resonant processes made it possible to increase the photon flux of such harmonics. This behavior was systematically analyzed using various materials [4]. The use of LIP allows analyzing the ionic transitions with high oscillator strength (i.e., high gf values that are the product of the oscillator strength f of the atomic transition and the statistical weight g of the lower level).

A breakthrough in this area of research has been demonstrated in the indium plasma, where a strong resonant increase in the conversion efficiency for a single harmonic ($>10^{-5}$) from a low-ionized LIP was experimentally achieved. The main effort so far has been to increase the photon flux of resonant harmonics. However, only a few studies have been conducted to better understand the physics associated with this generation of resonant harmonics. These experiments in different plasmas showed that the intensity of the resonant harmonics strongly depends on the ellipticity of the driving laser and follows the phase-matching conditions [5].

Most studies of HHG from LIP have so far focused on monatomic species [6–26], although HHG from diatomic molecules may offer some advantages due to their expanded structure and delocalized π electrons [27]. While single atoms with their relatively low ionization potentials probably limit HHG to low orders of generating harmonics, this is not obvious for the molecular species possessing higher ionization saturation intensities.

Such molecular structures can have their own transitions, which can be used for resonant amplification of the non-linear optical response in plasmas. In addition, they can shift some of the transitions responsible for harmonic amplification in the LIP containing the components of these molecules. Demonstration of this phenomenon can show the advantages of high-order non-linear spectroscopic analysis of molecular transitions whose oscillator strengths have not yet been studied. The reason for this assumption is related to the modification of the properties of ionic transitions under consideration. In particular, a decrease of the oscillator strength of some transitions responsible for enhancement of single harmonic may correlate with the replacement of the atomic Zn-contained plasma (i.e., the one produced on the bulk Zn target) by the molecular Zn-contained plasma (i.e., the one produced on the bulk ZnSe target). Our studies show that this assumption is more reliable compared with the tuning of the ionic transition responsible for harmonic enhancement to explain the observed decay in single harmonic amplification in molecular plasma.

The relative role of atomic and molecular transitions in HHG resonance amplification is still unclear. To clarify this problem, it is necessary to study the generation of harmonics from the ionized molecules and atoms containing same element using different laser sources allowing the spectral tuning of the driving field. This approach is important from the point of view of the probability of molecular decay in laser plasma with subsequent participation of its components in HHG.

Changing the excitation of certain substances can lead to some additional excited states that can amplify neighboring harmonics. Among different types of ablated substances, zinc-containing plasma can be considered an interesting object of study, since it allows varying the excitation of various AIS depending on the ablation conditions of the bulk target [28,29]. Target excitation makes it possible to analyze the non-linear response of such LIPs by comparing the amplification of different harmonics, provided that they coincide or remain close to these autoionizing states.

Initially, the role of Zn ion resonances near the 9th (H9) and 10th (H10) harmonics of the titanium sapphire laser was analyzed in [28,29]. However, the crucial role of strong ion transitions in more complex systems than zinc atoms is still questionable. Here we show how the single harmonic enhanced in the case of atomic plasma completely lost this peculiarity of harmonic amplification once the zinc becomes a component of the molecular cloud produced during laser ablation. We demonstrate the variations of single harmonic enhancement during single-color and two-color pumps of the zinc-containing plasmas using different laser sources.

2. Materials and Methods

Bulk zinc (Zn) metal and zinc selenide (ZnSe) targets were used in these studies. To create plasma, we used the Ti:sapphire laser (central wavelength 806 nm, pulse duration of uncompressed radiation 370 ps, pulse energy 4 mJ, 10 Hz pulse repetition rate). Part of the amplified uncompressed radiation was used as a heating pulse for LIP formation (Figure 1). The intensity and fluence of the heating pulse on the target surface were varied up to $I = 4 \times 10^9 \text{ W cm}^{-2}$ and $F = 2 \text{ J cm}^{-2}$, respectively. The ablation area was $0.6 \times 0.6 \text{ mm}^2$. In the case of single-color pump (SCP) of LIP, the focused compressed 806 nm, 64 fs, 10 Hz pulses (with 120 μm focal spot sizes and intensity varying in the range of $1.5 \times 10^{14} \text{ W cm}^{-2}$ and $4 \times 10^{14} \text{ W cm}^{-2}$) from this laser were aligned to propagate through plasma 0.2 mm above the ablating target. The 0.2-mm-thick beta-barium borate (BBO, type I) crystal was inserted into the vacuum chamber in the path of the 806 nm focused radiation (Figure 1) to generate harmonics using a two-color pump (TCP, 806 nm + 403 nm).

Optical parametric amplifier (OPA) was used to analyze the tuning of near infrared (NIR) radiation during HHG in Zn-contained plasmas. Most of the experiments using this laser source were carried out using the 1 mJ, 70 fs signal pulses tunable in the range of 1280–1440 nm. OPA pulses were focused on the plasma from the orthogonal direction. The intensity of the 1310 nm pulses focused by 400 mm focal length lens inside the plasma was $2 \times 10^{14} \text{ W cm}^{-2}$. Most of the experiments using OPA were carried out using TCP of LIP.

The 0.5 mm-thick BBO crystal (type I, $O = 21^\circ$) was installed inside the vacuum chamber on the path of focused signal pulses. The conversion efficiency of H2 pulses was 12%.

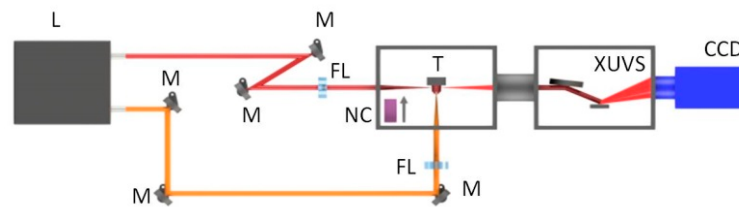


Figure 1. Experimental setup for high-order harmonic generation (HHG) in zinc-contained plasmas. L: laser; M: mirrors; FL: focusing lenses; NC: nonlinear crystal; T: target; XUVS: extreme ultraviolet spectrometer; CCD: charge-coupled device.

We used two orthogonally polarized pumps in the case of TCP of studied plasmas. Each of these pump components generate harmonics, while the mixture of pumps provided the $4(n+1)$ orders (H12, H16, H20, H24, etc.). Application of second field (i.e., second harmonic of the main pump) even at the low ratio of 2ω and ω waves allows the enhancement of the overall conversion efficiency of harmonics, as well as generation of even orders. The mechanism of such enhancement in the case of TCP is due to selection of a short quantum path component, which has a denser electron wave packet, and higher ionization rate compared with the SCP [30]. We maintained a suitable delay between fundamental and second fields in LIP by using thin BBO crystals.

An extreme ultraviolet spectrometer (XUVS) was used for the analysis of plasma and harmonic emission. The driving pulses and harmonics were separated by a flat field grating in the XUV spectrometer. Highest harmonic efficiency from LIP was observed at 100 or 250 ns delay from the beginning of Zn or ZnSe targets ablation. The variation of the optimal delay between heating and driving pulses was attributed to different velocities of spreading plasmas from the targets of different elemental weight.

3. Results

Previously, a study of the generation of high-order harmonics from ablated diatomic molecules (InSb, GaAs) showed that the discrepancy between the calculated molecular spectra and the observed resonantly amplified harmonics was due to the significantly greater influence of the strong electric field of laser radiation on the dynamic modification of molecular spectra [31]. The Stark shift in the energy levels of diatomic molecules can be considered the main reason for the decrease in the efficiency of single harmonics compared to monatomic LIPs (In, As, Sb), where the gain of single harmonics was explained by the proximity of the harmonic wavelength and the ion transitions with a strong oscillator strength. Below we address different aspects of this problem using single-atomic (Zn) and diatomic (ZnSe) plasma media.

Different fluencies of 806 nm pulses were used for the analysis of plasma and harmonic emission from an ablated Zn target. The application of fluence $F = 1.7 \text{ J cm}^{-2}$ did not result in plasma emission in the XUV range. The growth of fluence ($F = 2 \text{ J cm}^{-2}$) led to the appearance of emissions from two transitions of Zn II (88.1 and 89.3 nm) in the vicinity of the 9th harmonic of 806 nm pulses (89.6 nm).

Figure 2 shows the spectra observed during the generation of high-order harmonics of 806 nm, 64 fs, 10 Hz laser source in the case of ablation of zinc and zinc selenide bulk targets. In zinc plasma with optimal fluence of heating radiation ($F = 2 \text{ J cm}^{-2}$, upper panel), a $6\times$ -fold gain of ninth harmonic (H9) with regard to the neighboring (H7 and H11) harmonic orders was obtained. The observation of such an enhancement of the single harmonic cannot be attributed to the predominance of lower orders over higher ones at the beginning of the plateau-like range of the harmonic distribution. In our experiments, the lower harmonic (H7) was approximately six times weaker than H9. In the meantime,

the application of different plasmas (Ag, Au, Mo, etc.) showed that H9 was approximately equal to H7.

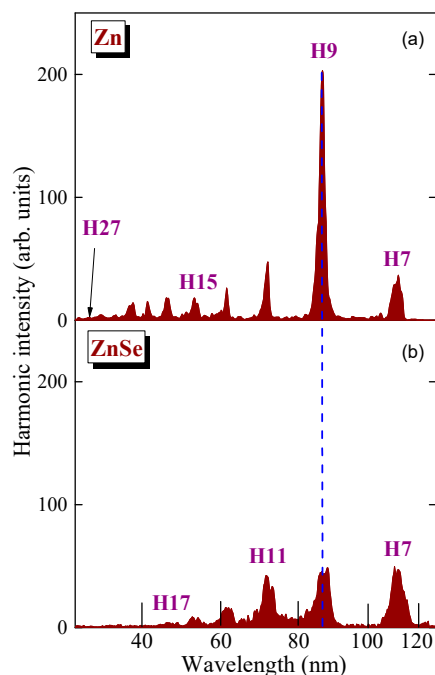


Figure 2. HHG from Zn-containing components of laser-induced plasma (LIP) using 806 nm driving pulses. Targets were ablated by 370 ps pulses. (a) Harmonic spectrum generated in Zn plasma using the fluence of heating $F = 2 \text{ J cm}^{-2}$. (b) Harmonic spectrum generated in ZnSe plasma ($F = 2.3 \text{ J cm}^{-2}$). Dashed line shows the position of $3d^{10}4s-3d^9 4s4p$ transition. H7–H27 correspond to the harmonic orders.

The wavelength of H9 ($\lambda = 89.6 \text{ nm}$) lies close to the Zn II transition ($3d^{10}4s-3d^9 4s4p$, 89.3 nm). Increasing the fluence of the heating pulses did not lead to disappearance of the resonance-related amplification effect, while reducing the gain of this harmonic. The maximum achieved harmonic cut-off under these conditions was H37 (not shown in the upper panel of Figure 2).

The application of ZnSe plasma for HHG significantly changed the envelope of the harmonic spectra (bottom panel of Figure 2) compared to that obtained from Zn ablation. Here we show the spectrum of harmonics obtained under optimal plasma formation conditions on the ZnSe bulk surface ($F = 2.3 \text{ J cm}^{-2}$). The term “optimal plasma formation” refers to the highest harmonic output from this LIP. One can see a featureless, gradually decreasing harmonics starting from H7 up to the cut-off range (H17 for ZnSe).

In Figure 2, we included the lines marking the position of the transition ($3d^{10}4s-3d^9 4s4p$, 89.3 nm [32]) responsible for the enhancement of single harmonic in Zn LIP. To further distinguish a difference between the HHG spectra from two plasmas under consideration, we included the same line in other figures (Figures 3 and 4) as well. Also note the observed closeness of two $3d^{10}4s-3d^9 4s4p$ transitions of Zn II (88.1 and 89.3 nm) with a wavelength of 9th harmonic ($\lambda = 89.6 \text{ nm}$) of 806 nm driving radiation. The enhancement of this harmonic has numerically been determined in [29].

The application of tunable NIR pulses from OPA allowed demonstration of the variation of single harmonic enhancement in the zinc plasma. Figure 3 shows four spectra of harmonics generated using different driving pulses (1280, 1320, 1380, and 1420 nm) and their second harmonics. The application of a 1280 nm + 640 nm pump did not allow generation of enhanced harmonics in the vicinity of strong ZnII transition (89.3 nm) marked by green dashed line (left upper panel). The nearest harmonic (H14) was not enhanced compared with the neighboring harmonic orders due to the detuning out from

the above transition. The shift of the wavelength of driving pulses towards 1340 nm allowed observing very strong H15 ($\lambda = 89.3$ nm) coinciding with the strong 89.3 nm ionic transition (right upper panel). Other odd and even orders were 3 to 7 times weaker than the resonance-enhanced harmonic.

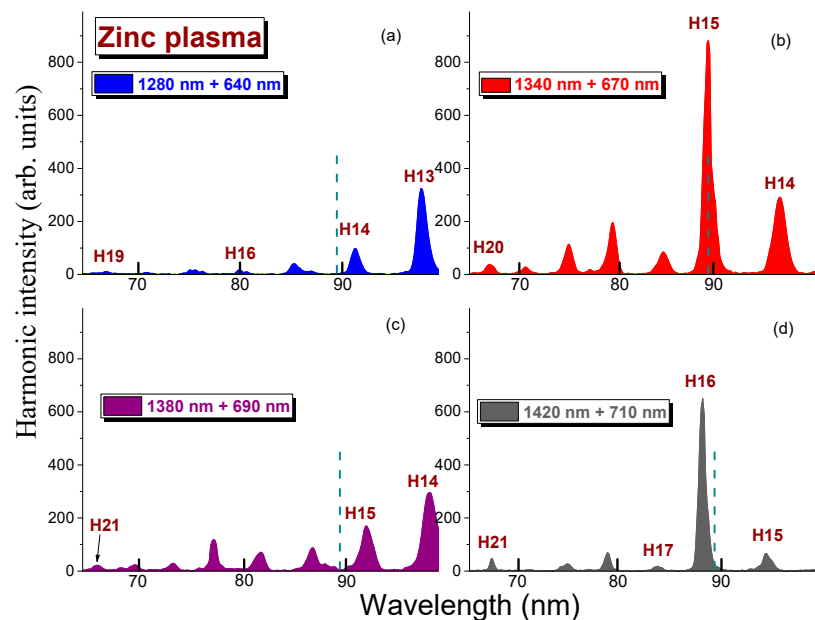


Figure 3. Harmonic spectra obtained during propagation of spectrally tunable pulses through the zinc LIP. A two-color pump (TCP) was used for determination of the resonantly enhanced harmonic orders matching with the wavelength of strong ZnII transition (89.3 nm, dashed line). Four groups of HHG spectra were obtained using (a) 1280 nm + 640 nm, (b) 1340 nm + 670 nm, (c) 1380 nm + 690 nm, and (d) 1420 nm + 710 nm pumps. Dashed lines show the position of the $3d^{10}4s-3d^94s4p$ transition. H14–H21 correspond to the harmonic orders.

Further shift of the driving wavelength towards the longer wavelength range (1380 nm, bottom left panel) again resulted in detuning of neighboring harmonics (H15 and H16) out from the position of resonance (dashed line). Finally, the application of 1420 nm emission and its second harmonic (bottom right panel) again created conditions for enhancement of the single harmonic. In that case the even (H16) harmonic was enhanced due to closeness with the ionic transition. Thus our studies using different lasers showed the enhancement of single harmonic once the conditions of closeness of the transition possessing strong oscillator strength and some harmonic order. In the case of the laser with fixed wavelength of driving pulses ($\lambda = 806$ nm), the enhancement of the single harmonic (Figure 2, upper panel) was similar to the one shown in Figure 3 using properly tuned wavelength of the driving field (see the spectra obtained at 1340 nm + 670 nm and 1420 nm + 710 nm).

Another pattern was observed in the case of ZnSe LIP. The tuning of the driving pulses between 1320 and 1440 nm in the case of TCP of this plasma caused a shift of harmonic wavelengths (see inclined dashed curves in Figure 4). However, the envelope of the harmonic distribution was approximately similar in each of these cases. No enhancement of the harmonics approaching the $\lambda = 89.3$ nm was observed. These experiments were carried out using the fluence of heating 370 ps pulses $F = 2.3$ J cm⁻². We modified conditions of experiments by either increasing the fluence of heating pulses up to the value when no strong plasma emission appears ($F = 3$ J cm⁻²), or increasing the intensity of driving pulses; however, no strong coherent emission in the vicinity of 90 nm was observed. Notice a similarity and gradual decrease of odd and even harmonics, which shows the sufficient overlap of NIR and second harmonic pulses in the plasma area in spite of using relatively thick non-linear crystal for the formation of a second field.

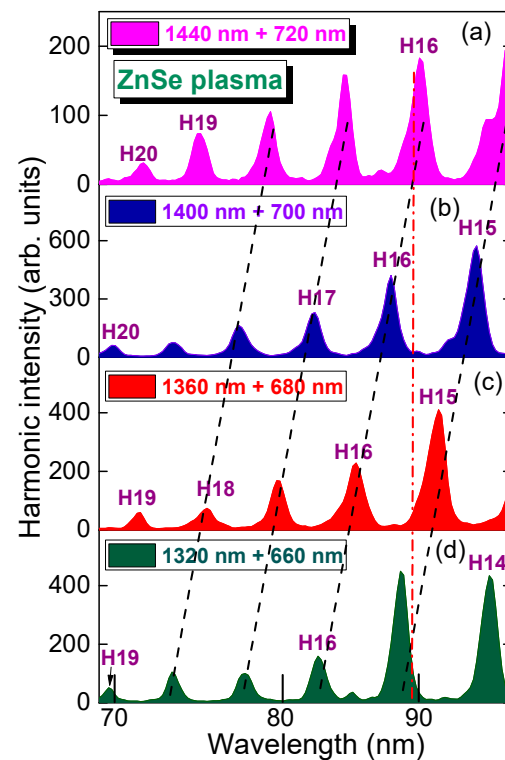


Figure 4. Harmonics generation in ZnSe plasma using the tunable NIR pulses. The wavelength of driving pulses was gradually tuned between 1320 and 1440 nm. No enhancement of odd and even harmonics in the vicinity of 89.3 nm was observed. Inclined dashed lines show the tuning ranges of odd and even harmonics. H14–H20 correspond to the harmonic orders. Dash-dotted line shows the position of the $3d^{10}4s-3d^94s4p$ transition. The two-color pump schemes were used during these studies with the following wavelengths of the interacting pulses: (a) 1440 nm and 720 nm, (b) 1400 nm and 700 nm, (c) 1360 nm and 680 nm, and (d) 1320 nm and 660 nm.

Numerous experiments using pulses in different time scales (between 4 and hundreds of femtoseconds) have shown the efficiency of harmonics generation in LIPs. Spectral broadening in the case of ultrashort pulses allows generation of subfemtosecond pulses during HHG in plasmas. In particular, the application of the few-cycle pulses for HHG in LIPs allowed almost entire suppression of surrounding harmonics during resonance enhancement of the notably broadened single (33rd) harmonic in the manganese plasma [33].

We did not measure the harmonic yield during these studies. Previously, different methods, like application of the photodiodes calibrated in XUV range, calibration of microchannel plate using the measurements of luminescence in different spectral ranges, etc., were implemented to quantitatively determine the harmonic yield from different plasmas. Those quantitative measurements of harmonic yield still suffer in accuracy, though some comparative estimates and measurements show that harmonics generation in plasma is at least a few times higher than in gases at similar experimental conditions. Although it is difficult to compare harmonic data in the case of different facilities, the conversion efficiency up to 10^{-5} was reported in the case of silver plasma. Even higher conversion efficiencies were reported in the case of a resonantly enhanced single harmonic in indium plasma, as well as harmonics generating in nanoparticle-containing LIPs. In our case we estimated the 10^{-6} conversion efficiency in the plateau range of harmonic distribution, while the resonant harmonics were up to 10 times stronger (i.e., their conversion efficiency was in the range of 10^{-5}).

4. Discussion

The following characteristics of two studied materials related to the topics of present studies can cause a difference in the harmonic emission. Zinc is a chemical element belonging to the transition metals with the atomic weight 66. Its electron configuration ($3d^{10} 4s^2$) coincides with Ar. Other important parameters are the melting point (~ 700 K), boiling point (~ 1200 K), heat of fusion and vaporization (7.3 and 115 kJ/cm⁻³), and ionization energies (1st: 906.4 kJ/mol, 2nd: 1733.3 kJ/mol, 3rd: 3833 kJ/mol). Zinc selenide is a light-yellow, solid compound comprising zinc (Zn) and selenium (Se) with the atomic weight 144. ZnSe can be made in both hexagonal and cubic crystal structure. It is a wide-bandgap semiconductor of the II-VI semiconductor group (since zinc and selenium belong to the 12th and 16th groups of the periodic table, respectively). Its melting point and band gap are ~ 1800 K and 2.8 eV, respectively. Our studies showed that zinc ablates at lower fluence compared with zinc sulfide. Nevertheless, in spite of the difference in the physical properties of these two solids, the ablation at optimal fluence of each of these materials allowed generation of harmonics with approximately similar conversion efficiency. The main distinction between two HHG spectra from those plasmas is related to the envelopes of harmonic distribution (compare Figures 2–4) demonstrating the resonance effect in the case of atomic plasma.

There are no data to the best of our knowledge on the ZnSe transitions in the XUV range possessing large *gfs*, especially in the vicinity of the harmonics of either fixed (806 nm) or tunable NIR pumps. The unavailability of this information does not tell us conclusively about their absence. They may either be lower than that responsible for the enhancement of a single harmonic generating in atomic/ionic Zn plasma in the vicinity of 90 nm, or can be tuned out from the initial position assigned in the case of atomic medium. The most probable reason is the former since the latter assumption was analyzed by tuning the pump wavelength in the case of a tunable NIR source (Figure 4), while no enhancement of harmonic, contrary to that observed in the case of ablated zinc (Figure 3), was achieved.

The cutoffs of the harmonics generating in zinc selenide plasma were in the range of ~ 50 nm in the case of the 806 nm pump (Figure 2) and 60 nm in the case of the 1400 nm + 700 nm pump (not shown in Figure 4). The discrepancy between the experiment and the expectations in the extension of this parameter for the longer-wavelength pump ($E_{\text{cutoff}} \propto \lambda^2$, E_{cutoff} is the harmonic cutoff and λ is the driving field wavelength) can be attributed to the difference in the beam sizes in plasma area and smaller conversion efficiency in the case of tunable NIR pulses. We recall that the efficiency of the harmonics produced by shorter wavelength source becomes higher due to the strong wavelength-dependent yield ($I_{\text{harm}} \propto \lambda^{-5}$ [34]; I_{harm} is the harmonic intensity).

There are a number of theoretical approaches that describe the effect of resonance on the microscopic and macroscopic response of atomic medium leading to the enhancement of a single harmonic [3,35–43]. However, the mechanism of this resonant amplification in atomic medium is still debatable. There are two possible approaches: one relies on a better recombination cross-section through the AIS in a single-atom response, and the other relies on the improved phase matching conditions in the vicinity of the resonance. Which of them provides stronger influence on the unusual distribution of harmonics depends on the medium used, laser pump conditions, and coincidence of harmonic and ionic transition wavelength, as well as the oscillator strengths of those transitions. Another additional factor, as our studies show, is the elemental consistence of plasma components.

Below we briefly address the above issues and qualitatively compare different theoretical approaches described in theoretical studies and our results. We did not include the quantitative comparison with the theory of resonance enhancement of the single harmonic of Ti:sapphire laser during propagation of femtosecond plasmas through the atomic/ionic zinc LIP, since such a theoretical analysis has already been published elsewhere [29]. Note that similar quantitative analysis of the resonance-induced HHG in some other atomic plasmas ([3,35,39,40] in the case of in plasma and [3,35,44] in the case of Cr plasmas).

For different theoretical approaches offered in those studies the common important peculiarity is that the harmonic wavelength is resonant with the transition between the ground and the autoionizing state (i.e., the excited state embedded in the continuum) of the generating ion and that this transition exhibits high oscillator strength. In particular, in the so-called four-step model [3] the ionized and laser-accelerated electron is captured into the AIS of the parent ion, and, in the final step, the radiative relaxation of this state to the ground state, a harmonic photon is emitted. Another approach [35,45] generalized to the case of a bichromatic laser field with orthogonally polarized components can also be used for determination of the peculiarities of resonance enhancement using a two-color pump. In the model further developed in [44] the capture into an AIS is replaced by the field-induced excitation of the ground state into this state and the harmonic strength consists of both resonant and non-resonant parts. It was assumed that the target material is such that there is a high radiative transition probability between the ground state with energy $E1$ and a low-lying state having energy $E2$. If the laser frequency is such that the condition $\Delta\omega = E2 - E1 = nR\omega$, where nR is the integer, is fulfilled, then, during the single-state HHG process, a coherent superposition of the ground state and this excited state will be formed.

Summarizing, the existing theories of the microprocess of resonance-induced enhancement of a single harmonic in atomic plasmas are mostly based on (i) the four-step model, (ii) the harmonic generation in the presence of a shape resonance using time-frequency analysis of the intensity and phase, which underlined the resonance enhancement irrespective of the pulse length and supported the four-step model, and (iii) the approach generalized for the case when the capture into an AIS is replaced by the field-induced excitation of the ground state into this state. The usual three-step scenario that applies the factorization formula without additional assumptions [37] also provides explanation of the earlier reported resonance-enhanced processes in different LIPs, as well as those studied in present research of atomic Zn plasmas. The variation of target excitation broadens analysis of the non-linear response of such plasma by comparing the enhancement of different harmonics provided they coincide or stay close to those resonances. In particular, the application of this approach during numerical study of HHG in Zn ions allowed the resonance effect in harmonic generation to be observed due to transitions to the highly excited bound states, rather than to the AIS [29]. However, these bound states are broader due to photoionization in the intense laser field. Thus in this sense there is no fundamental difference between transitions to AIS (enhancing above-ionization threshold harmonics) and transitions to highly excited bound states (enhancing below-threshold harmonics). Moreover, the generation of the below-threshold harmonics also includes the quasi-free electronic motion as one of the steps of the process, and therefore the resonant enhancement of this generation can be described within the similar four-step model. One has to take into consideration the opportunity in competition of the micro- and macro-processes in the LIP. In particular, the comparison of the quasi-phase matching and resonance enhancement of harmonics using TCP of plasmas has been demonstrated and discussed in [46].

Notice that the aforementioned resonance enhancement has clearly been demonstrated both experimentally and theoretically only in the case of atomic plasmas. Meanwhile, the application of the molecular plasmas contained the components responsible for amplification process did not result in resonantly-enhanced single harmonic, in spite of the attempts to decay and disintegrate molecules like ZnSe. Previous calculations of modified spectra of some plasma plumes were performed to distinguish the level of detuning and the mechanisms that lead to a decrease in the amplification of a specific harmonic order in the case of a molecular plume with respect to an atomic one [47]. The discrepancy between the calculated spectra and the experimentally observed less effective resonant-amplified harmonics in semiconductor molecules compared with atomic/ionic plumes was explained by a significantly greater influence of the strong electric field of laser radiation on the symmetry and dynamic modification of the molecular spectra in LIP.

In previous simulations of HHG from LIP [40], an effective Coulomb potential (e.g., soft-core potential) was adopted to mimic the target. For the zinc plasma reported in the present study, one can choose a similar method as the previous work [40], and strong emission can be obtained in the simulations. On the other hand, in principle, one should also choose the similar method for ZnSe. However, in the case of similar potential, the same strong emission of single harmonic from above molecular LIPs is anticipated which is in contrast with our experiment. To explain our experimental findings on molecular zinc-contained plasmas, more sophisticated theory such as density functional theory will be needed to accurately simulate the target structures and dynamics.

Our experimental results in the case of atomic Zn plasma well match with the theoretical consideration of this process described in the above refereed theoretical studies independent of the wavelength of the pumping laser, thus confirming the generalized approach of those theoretical studies. In particular, note the observed closeness of two $3d^{10}4s-3d^94s4p$ transitions of Zn II (88.1 and 89.3 nm) with a wavelength of the 9th harmonic of 806 nm driving radiation. The enhancement of this harmonic was numerically determined in [29]. These transitions also influenced the harmonic yield in the case of our HHG in Zn plasma using 1340 nm (H15) and 1420 nm (H16) pump radiation (Figure 3). Those harmonics (H15 and H16), being positioned near the above ionic transitions of singly-ionized zinc, were enhanced compared with the neighboring ones thus confirming the theoretical prediction [29].

Our experimental studies clearly show the difference in the harmonic spectra from the plasmas comprising the atomic and molecular species of the same elemental structure of metal ingredient. One can assume that the molecular spectra change with regard to the spectra of ionized atoms, which leads to the detuning of known transitions with strong oscillator strengths out from a specific harmonic wavelength. Thus the efficient resonance processes during HHG may occur when the ablated plasma comprises the atoms rather than molecules. In particular, it is unlikely that the presence of atomic ions in the studied molecular plasmas, such as zinc selenide, can under certain conditions lead to the resonance-enhanced HHG. We showed that selenides of this metal noticeably reduce the amplification of single harmonic in comparison with purely atomic plasmas due to either the displacement of ion transitions with strong oscillator strengths beyond the wavelength of these harmonics or the decrease of their gfs in the molecular state of the ZnSe case. Meanwhile, disintegration of zinc selenide during strong ablation of the target did not allow demonstration of resonance effect, while maintaining suitable conditions of the phase matching in over-excited LIP.

The absence of resonance enhancement in ZnSe points out the diminished role of the spectrally shifted transition in this process. The detuning of this transition in the case of molecules out from the atomic transition can be compensated for by tuning the wavelength of harmonic, as in the case of our experiments with the OPA pumping system. However, these experiments showed that the fine tuning of the harmonic along the expected strong transition did not result in the enhancement of some specific harmonics in the vicinity of this resonance (Figure 4). Our attempt to decay and disintegrate this molecule at higher fluencies ($F = 3 \text{ J cm}^{-2}$), did not result in the enhancement of the single harmonic caused by the presence of a sufficient amount of Zn ions in such a plasma. Stronger fluencies ($F = 3.5 \text{ J cm}^{-2}$) caused the intense emission of incoherent radiation from plasma, as well as the formation of a large amount of free electrons, which fully destroy the phase matching conditions, especially for the higher orders of harmonics.

5. Conclusions

We have reconsidered the mechanism of resonant amplification of single harmonic in zinc-containing atomic and molecular plasmas when generating high-order harmonics in laser plasma plumes. It has been shown that selenides of this metal noticeably reduce the amplification of the single harmonic in comparison with purely atomic plasmas, probably due to the decrease of the oscillator strength of the involved ionic transitions. Stronger

ablation of these molecular targets did not allow the resonant amplification of the single harmonic in ZnSe plasma to be restored using different laser sources, probably due to the insufficient decay of molecules leading to the appearance of zinc ions.

Our research allows us to predict modification of the mechanism of resonant amplification of single harmonics reported in other atomic plasmas (manganese, tin, chromium, selenium, tellurium, molybdenum, indium, and arsenic) being presented in the molecular form. This process can also be reconsidered by comparing the atomic and molecular plasmas containing the above elements, as well as by tuning the wavelength of driving radiation along those resonances that are responsible for the observed amplification of harmonics.

Author Contributions: Conceptualization, R.A.G., H.K.; methodology, R.A.G.; formal analysis, R.A.G., H.K.; investigation, R.A.G., H.K.; writing—original draft preparation, R.A.G.; writing—review and editing, R.A.G., H.K.; visualization, R.A.G.; supervision, H.K.; funding acquisition, R.A.G., H.K. All authors have read and agreed to the published version of the manuscript.

Funding: This work was supported by JSPS KAKENHI (24760048), ERDF project (1.1.1.5/19/A/003), State Assignment to Higher Educational Institutions of Russian Federation (FZGU-2020-0035).

Institutional Review Board Statement: Not applicable.

Informed Consent Statement: Not applicable.

Data Availability Statement: The data that support the findings of this study are available from the corresponding author upon reasonable request.

Conflicts of Interest: The authors declare no conflict of interest.

References

1. Ganeev, R.A.; Suzuki, M.; Baba, M.; Kuroda, H. Harmonic generation in XUV from chromium plasma. *Appl. Phys. Lett.* **2005**, *86*, 131116. [[CrossRef](#)]
2. Ganeev, R.A.; Singhal, H.; Naik, P.A.; Arora, V.; Chakravarty, U.; Chakera, J.A.; Khan, R.A.; Redkin, P.V.; Raghuramaiah, M.; Gupta, P.D. Single harmonic enhancement by controlling the chirp of the driving laser pulse during high-order harmonic generation from GaAs plasma. *J. Opt. Soc. Am. B* **2006**, *23*, 2535. [[CrossRef](#)]
3. Strelkov, V. Role of autoionizing state in resonant high-order harmonic generation and attosecond pulse production. *Phys. Rev. Lett.* **2010**, *104*, 123901. [[CrossRef](#)]
4. Ganeev, R.A. *Resonance Enhancement in Laser-Produced Plasmas: Concepts and Applications*; Wiley: Hoboken, NJ, USA, 2018.
5. Suzuki, M.; Baba, M.; Ganeev, R.; Kuroda, H.; Ozaki, T. Anomalous enhancement of single high-order harmonic using laser ablation tin plume at 47 nm. *Opt. Lett.* **2006**, *31*, 3306. [[CrossRef](#)]
6. Ganeev, R.A.; Elouga Bom, L.B.; Wong, M.C.H.; Brichta, J.-P.; Bhardwaj, V.R.; Redkin, P.V.; Ozaki, T. High-order harmonic generation from C₆₀-rich plasma. *Phys. Rev. A* **2009**, *80*, 043808. [[CrossRef](#)]
7. Singhal, H.; Arora, V.; Rao, B.S.; Naik, P.A.; Chakravarty, U.; Khan, R.A.; Gupta, P.D. Dependence of high-order harmonic intensity on the length of preformed plasma plumes. *Phys. Rev. A* **2009**, *79*, 023807. [[CrossRef](#)]
8. Singhal, H.; Ganeev, R.A.; Naik, P.A.; Srivastava, A.K.; Singh, A.; Chari, R.; Khan, R.A.; Chakera, J.A.; Gupta, P.D. Study of high-order harmonic generation from nanoparticles. *J. Phys. B At. Mol. Opt. Phys.* **2010**, *43*, 025603. [[CrossRef](#)]
9. Pertot, Y.; Elouga Bom, L.B.; Bhardwaj, V.R.; Ozaki, T. Pencil lead plasma for generating multimicrojoule high-order harmonics with a broad spectrum. *Appl. Phys. Lett.* **2011**, *98*, 101104. [[CrossRef](#)]
10. Sheinfux, H.; Hems, Z.; Levin, M.; Zigler, A. Plasma structures for quasiphase matched high harmonic generation. *Appl. Phys. Lett.* **2011**, *98*, 141110. [[CrossRef](#)]
11. Elouga Bom, L.B.; Pertot, Y.; Bhardwaj, V.R.; Ozaki, T. Multi- μ J coherent extreme ultraviolet source generated from carbon using the plasma harmonic method. *Opt. Express* **2011**, *19*, 3077. [[PubMed](#)]
12. Hutchison, C.; Ganeev, R.A.; Witting, T.; Frank, F.; Okell, W.A.; Tisch, J.W.G.; Marangos, J.P. Stable generation of high-order harmonics of femtosecond laser radiation from laser produced plasma plumes at 1 kHz pulse repetition rate. *Opt. Lett.* **2012**, *37*, 2064. [[CrossRef](#)] [[PubMed](#)]
13. Haessler, S.; Elouga Bom, L.B.; Gobert, O.; Hergott, J.-F.; Lepetit, F.; Perdrix, M.; Carré, B.; Ozaki, T.; Salières, P. Femtosecond envelope of the high-harmonic emission from ablation plasmas. *J. Phys. B At. Mol. Opt. Phys.* **2012**, *45*, 074012. [[CrossRef](#)]
14. Ganeev, R.A.; Hutchison, C.; Witting, T.; Frank, F.; Okell, W.A.; Zair, A.; Weber, S.; Redkin, P.V.; Lei, D.Y.; Roschuk, T.; et al. High-order harmonic generation in graphite plasma plumes using ultrashort laser pulses: A systematic analysis of harmonic radiation and plasma conditions. *J. Phys. B At. Mol. Opt. Phys.* **2012**, *45*, 165402. [[CrossRef](#)]

15. Pertot, Y.; Chen, S.; Khan, S.D.; Elouga Bom, L.B.; Ozaki, T.; Chang, Z. Generation of continuum high-order harmonics from carbon plasma using double optical gating. *J. Phys. B At. Mol. Opt. Phys.* **2012**, *45*, 074017. [[CrossRef](#)]
16. Kumar, M.; Singhal, H.; Chakera, J.A.; Naik, P.A.; Khan, R.A.; Gupta, P.D. Study of the spatial coherence of high order harmonic radiation generated from preformed plasma plumes. *J. Appl. Phys.* **2013**, *114*, 033112. [[CrossRef](#)]
17. Ganeev, R.A.; Suzuki, M.; Kuroda, H. Quasi-phase-matching of high-order harmonics in multiple plasma jets. *Phys. Rev. A* **2014**, *89*, 033821. [[CrossRef](#)]
18. Singhal, H.; Naik, P.A.; Kumar, M.; Chakera, J.A.; Gupta, P.D. Enhanced coherent extreme ultraviolet emission through high order harmonic generation from plasma plumes containing nanoparticles. *J. Appl. Phys.* **2014**, *115*, 033104. [[CrossRef](#)]
19. Rosenthal, N.; Marcus, G. Discriminating between the role of phase matching and that of the single-atom response in resonance plasma-plume high-order harmonic generation. *Phys. Rev. Lett.* **2015**, *115*, 133901. [[CrossRef](#)]
20. Fareed, M.A.; Thiré, N.; Mondal, S.; Schmidt, B.E.; Légaré, F.; Ozaki, T. Efficient generation of sub-100 eV high-order harmonics from carbon molecules using infrared laser pulses. *Appl. Phys. Lett.* **2016**, *108*, 124104. [[CrossRef](#)]
21. Fareed, M.A.; Strelkov, V.V.; Thiré, N.; Mondal, S.; Schmidt, B.E.; Légaré, F.; Ozaki, T. High-order harmonic generation from the dressed autoionizing states. *Nat. Commun.* **2017**, *8*, 16061. [[CrossRef](#)]
22. Wöstmann, M.; Splittthoff, L.; Zacharias, H. Control of quasi-phase-matching of high-harmonics in a spatially structured plasma. *Opt. Express* **2018**, *26*, 14524. [[CrossRef](#)] [[PubMed](#)]
23. Fareed, M.A.; Strelkov, V.V.; Singh, M.; Thiré, N.; Mondal, S.; Schmidt, B.E.; Légaré, F.; Ozaki, T. Harmonic generation from neutral manganese atoms in the vicinity of the giant autoionization resonance. *Phys. Rev. Lett.* **2018**, *121*, 023201. [[CrossRef](#)] [[PubMed](#)]
24. Abdelrahman, Z.; Khohlova, M.A.; Walke, D.J.; Witting, T.; Zair, A.; Strelkov, V.V.; Marangos, J.P.; Tisch, J.W.G. Chirp-control of resonant high-order harmonic generation in indium ablation plumes driven by intense few-cycle laser pulses. *Opt. Express* **2018**, *26*, 15745. [[CrossRef](#)] [[PubMed](#)]
25. Kumar, M.; Singhal, H.; Chakera, J.A. High order harmonic radiation source for multicolor extreme ultraviolet radiography of carbon plumes. *J. Appl. Phys.* **2019**, *125*, 155902. [[CrossRef](#)]
26. Singh, M.; Fareed, M.A.; Laramée, A.; Isgandarov, E.; Ozaki, T. Intense vortex high-order harmonics generated from laser-ablated plume. *Appl. Phys. Lett.* **2019**, *115*, 231105. [[CrossRef](#)]
27. Mairesse, Y.; Levesque, J.; Dudovich, N.; Corkum, P.B.; Villeneuve, D.M. High harmonic generation from aligned molecules amplitude and polarization. *J. Modern Opt.* **2008**, *55*, 2591. [[CrossRef](#)]
28. Ganeev, R.A.; Baba, M.; Suzuki, M.; Yoneya, S.; Kuroda, H. Low- and high-order harmonic generation in the extended plasmas produced by laser ablation of zinc and manganese targets. *J. Appl. Phys.* **2014**, *116*, 243102. [[CrossRef](#)]
29. Ganeev, R.A.; Suzuki, M.; Yoneya, S.; Strelkov, V.V.; Kuroda, H. Resonance enhancement of harmonics in laser-produced Zn II and Zn III containing plasmas using tunable mid-infrared pulses. *J. Phys. B At. Mol. Opt. Phys.* **2016**, *49*, 055402. [[CrossRef](#)]
30. Kim, I.J.; Kim, C.M.; Kim, H.T.; Lee, G.H.; Lee, Y.S.; Park, J.Y.; Cho, D.J.; Nam, C.H. Highly efficient high-harmonic generation in an orthogonally polarized two-color laser field. *Phys. Rev. Lett.* **2005**, *94*, 243901. [[CrossRef](#)]
31. Ganeev, R.A.; Naik, P.A.; Singhal, H.; Chakera, J.A.; Gupta, P.D. Strong enhancement and extinction of single harmonic intensity in the mid- and end-plateau regions of the high harmonics generated in low-excited laser plasmas. *Opt. Lett.* **2007**, *32*, 65. [[CrossRef](#)]
32. Crooker, A.M.; Dick, K.A. Extensions to the spark spectra of zinc. I. Zinc II and zinc IV. *Canad. J. Phys.* **1968**, *46*, 1241. [[CrossRef](#)]
33. Ganeev, R.A.; Witting, T.; Hutchison, C.; Frank, F.; Tudorovskaya, M.; Lein, M.; Okell, W.A.; Zair, A.; Marangos, J.P.; Tisch, J.W.G. Isolated sub-fs XUV pulse generation in Mn plasma ablation. *Opt. Express* **2012**, *20*, 25239. [[CrossRef](#)] [[PubMed](#)]
34. Lan, P.; Takahashi, E.; Midorikawa, K. Wavelength scaling of efficient high-order harmonic generation by two-color infrared laser fields. *Phys. Rev. A* **2010**, *81*, 061802. [[CrossRef](#)]
35. Milošević, D.B. High-energy stimulated emission from plasma ablation pumped by resonant high-order harmonic generation. *J. Phys. B At. Mol. Opt. Phys.* **2007**, *40*, 3367. [[CrossRef](#)]
36. Kulagin, I.A.; Usmanov, T. Efficient selection of single high-order harmonic caused by atomic autoionizing state influence. *Opt. Lett.* **2009**, *34*, 2616. [[CrossRef](#)]
37. Frolov, M.V.; Manakov, N.L.; Starace, A.F. Potential barrier effects in high-order harmonic generation by transition-metal ions. *Phys. Rev. A* **2010**, *82*, 023424. [[CrossRef](#)]
38. Redkin, P.V.; Ganeev, R.A. Simulation of resonant high-order harmonic generation in three-dimensional fullerene-like system by means of multiconfigurational time-dependent Hartree-Fock approach. *Phys. Rev. A* **2010**, *81*, 063825. [[CrossRef](#)]
39. Tudorovskaya, M.; Lein, M. High-order harmonic generation in the presence of a resonance. *Phys. Rev. A* **2011**, *84*, 013430. [[CrossRef](#)]
40. Ganeev, R.A.; Wang, Z.; Lan, P.; Lu, P.; Suzuki, M.; Kuroda, H. Indium plasma in the single- and two-color mid-infrared fields: Enhancement of tunable harmonics. *Phys. Rev. A* **2016**, *93*, 043848. [[CrossRef](#)]
41. Wahyutama, I.S.; Sato, T.; Ishikawa, K.L. Time-dependent multiconfiguration self-consistent-field study on resonantly enhanced high-order harmonic generation from transition-metal elements. *Phys. Rev. A* **2019**, *99*, 063420. [[CrossRef](#)]
42. Ngoko Djiokap, J.M.; Starace, A.F. Origin of the multiphoton-regime harmonic-generation plateau structure. *Phys. Rev. A* **2020**, *102*, 013103. [[CrossRef](#)]

43. Kim, V.V.; Boltaev, G.S.; Iqbal, M.; Abbasi, N.A.; Al-Harmi, H.; Wahyutama, I.S.; Sato, T.; Ishikawa, K.L.; Ganeev, R.A.; Alnaser, A.S. Resonance enhancement of harmonics in the vicinity of 32 nm spectral range during propagation of femtosecond pulses through the molybdenum plasma. *J. Phys. B At. Mol. Opt. Phys.* **2020**, *53*, 195401. [[CrossRef](#)]
44. Ganeev, R.A.; Odžak, S.; Milošević, D.B.; Suzuki, M.; Kuroda, H. Resonance enhancement of harmonics in metal plasmas using tunable mid-infrared pulses. *Laser Phys.* **2016**, *26*, 075401. [[CrossRef](#)]
45. Milošević, D.B. Resonant high-order harmonic generation from plasma ablation: Laser intensity dependence of the harmonic intensity and phase. *Phys. Rev. A* **2010**, *81*, 023802. [[CrossRef](#)]
46. Ganeev, R.A.; Boltaev, G.S.; Stremoukhov, S.Y.; Kim, V.V.; Andreev, A.V.; Alnaser, A.S. High-order harmonic generation during different overlaps of two-colored pulses in laser-produced plasmas. *Eur. Phys. J. D* **2020**, *74*, 199. [[CrossRef](#)]
47. Ganeev, R.A.; Redkin, P.V. Role of resonances in the high-order harmonic enhancement in diatomic molecules. *Opt. Commun.* **2008**, *281*, 4126. [[CrossRef](#)]